METABOLISM STUDIES OF HCA, QCN AND GLZ

4. Metabolism Studies of HCA, QCN and GLZ

4.1. Introduction

Metabolism involves the transformation of lipophilic drugs to a more hydrophilic moiety (metabolite) which promotes its elimination from the body. Metabolism has a greater impact on the drug distribution, toxicity and elimination of compounds [1]. The liver is the principal organ for xenobiotic metabolism [2]. Metabolism occurs primarily in two phases, *i.e.,* phase-I and phase-II. The phase-I metabolic reactions involve the conversion of lipophilic drug to hydrophilic moiety by reduction, oxidation and hydrolysis. These reactions involve the introduction or unmask of a polar functional group on the drug. Phase-I reactions primarily occur through cytochrome P450 (CYP) enzyme which are found in abundance in the liver [3]. The majority of drugs metabolized by the major CYP isoforms include the CYP3A4, CYP1A2, CYP2E1, CYP2C8, CYP2C9, CYP2C19, CYP2D6 and CYP2B6. The main enzyme involved in the phase-I metabolism is CYP3A4 and this enzyme represents ~ 30% of total CYP protein present in the liver. CYP3A4 has multiple active sites and is considered to be accountable for the metabolism of almost half of the marketed drugs [4]. The phase-II reaction involves the conjugation with a hydrophilic moiety such as glucuronic acid, sulfate, α- amino acids, glutathione, etc. The formed metabolite can be active, toxic and participate in the drug-drug interactions. In the early phase of drug discovery, compounds are usually screened for *in vitro* metabolic stability by using liver microsomes (LM) of different species. It will elucidate the metabolic pathway of a compound. This approach is widely preferred in industries to predict the *in vivo* clearance. Additionally, the metabolism due to non-CYP enzyme is tested by S9 fractions, hepatocytes, or cytosol [5]. The recombinant CYP or UGT isoforms are preferred to evaluate the specific enzyme responsible for metabolism [6]. The exploration of CYP responsible for metabolism is useful for the early prediction of drug-drug interactions (DDI) liabilities of a compound. CYP inhibition or induction is the main cause of DDI which limits the use of several combination therapies. Metabolite identification by HRMS is a well-established method to explore the formed metabolite(s). In the present studies, metabolic pathways of HCA, QCN and GLZ are evaluated by using freshly isolated rat liver S9 fractions and the possibility of CYP3A4 inhibition/induction was accessed.

4.2. *In-silico* analysis of metabolism of HCA, QCN & GLZ

In recent years, *in vitro* and *in vivo* pharmacokinetic prediction methods have been extensively used, but it is not always feasible to perform time-consuming, resource-intensive, complex and expensive pharmacokinetic experiments on a large number of compounds. Therefore, an *in silico* strategy to predict ADMET properties has become a high-throughput alternative and

cost-effective strategy. Molecular modeling (based on the three-dimensional structure of the protein) and data modeling {based on PBPK (physiologically-based pharmacokinetic) and QSAR (quantitative structure-activity relationship)} are the two *in silico* approaches that are used for ADMET prediction [7]. Molecular modeling includes multiple methods such as simulation, molecular docking and quantum mechanics (QM) calculation. Metabolism of HCA, QCN and GLZ was predicted using ADMET Predictor® from GastroPlus® software package (Simulations Plus, USA). Metabolism Module in ADMET Predictor® allows to predict:

- Site of metabolism and metabolites for 9 CYP isoforms
- K_m, V_{max}, CL_{int} (CYP kinetic parameters) and inhibition for the 5 major drug-metabolizing CYPs
- Unbound intrinsic clearance (Human and rat liver microsome)
- UGT substrate potential for 9 UGT isoforms

4.2.1. HCA

In-silico analysis of metabolism of HCA

The *in-silico* prediction of metabolites of HCA using ADMET Predictor® of GastroPlus® along with the depicted mass of potential metabolites through the listed enzymes is shown in Table 4.1

Table 4.1. Output of ADMET Predictor® for metabolite prediction of HCA.

Identifier	Metabolizing enzyme	Mass
HCA		208.126
HCA - M1	UGT1A3;UGT1A6	384.0534
HCA - M2	UGT2B7	384.0534
HCA - M3	UGT2B7	384.0534
HCA - M4	UGT2B7	384.0534

Glucuronidation through UGT2B7, UGT1A6 and UGT1A3 is predicted to be the key pathway for the metabolism of HCA. The prediction is due to the existence of three carboxylic acid groups that are known to undergo glucuronidation [8].

Metabolite Identification of HCA in RLS9

The incubation protocol is described in Section 3.4. Briefly, the final concentration of the protein was 1 mg/mL (RLS9 fraction), and HCA concentration was 10 μg/mL. Control incubations did not had HCA/NADPH. After a pre-incubation period of 5 minutes at 37 °C, addition of 2.0 mM NADPH cofactor solution instigated the metabolic reaction. Subsequent to the incubation for 60 minutes, 1 mL ice-cold acetonitrile was added to the reaction mixture to

quench the same, and the resultant samples were subjected to centrifugation at 10,000 rpm for 10 minutes before injecting on to the HRMS.

Mass Fragment Ions of HCA

Using HCA as the central core for its metabolites, the MS^2 fragment ions could be used as indicator towards metabolite identification. In the MS^2 mode, with the collision energy (CE) of 35 eV, HCA resulted in only one major fragment ion at *m/z* 127.0401 ($C_6H_7O_3$) Figure 4.1.

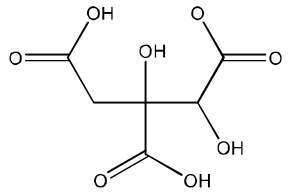

Chemical Formula: $C_6H_7O_8^-$
Exact Mass: 207.0146

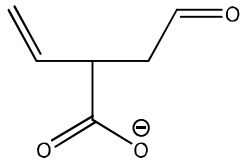

Chemical Formula: $C_6H_7O_3^-$
Exact Mass: 127.0401

Figure 4.1. Predicted (theoretical) mass fragmentation ions of HCA

Based on the m/z of HCA, the exact mass of the simulated metabolites is presented in Table 4.2. It provides a template for searching phase I and phase II metabolites of HCA from the obtained mass data. This mass list was used to acquire a data-dependent scan on HRMS.

Table 4.2. Exact mass (m/z) of the expected metabolites of HCA.

[M-H]-	**207.0146**		
Metabolism Reaction	**Formula change**	**Accurate mass change**	**Accurate mass**
ter-butyl dealkylation	($-C_4H_8$)	(-56.0626)	150.9521
Decarboxylation	($-CO_2$)	(-43.9898)	163.0248
Isopropyl dealkylation	($-C_3H_6$)	(-42.0473)	164.9676
Reductive dechlorination	(+H-Cl)	(-33.9611)	173.0536
Deethylation	($-C_2H_4$)	(-28.0313)	178.9833
Reductive defluorination	(+H-F)	(-17.9906)	189.0246
Oxidative dechlorination	(+OH-Cl)	(-17.9661)	189.0485
Demethylation	($-CH_2$)	(-14.0157)	192.9989
Two sequential desaturations	($-H_4$)	(-4.0313)	202.9833
Hydroxylation and dehydration	($-H_2$)	(-2.0157)	204.9989
Alcohol to ketone/aldehyde	($-H_2$)	(-2.0157)	204.9989
Desaturation	($-H_2$)	(-2.0157)	204.9989
Oxidative defluorination	(+OH-F)	(-1.9957)	205.0189
Oxidative deamination	($-NH_3$+O)	(-1.0316)	205.9831
Demethylation and hydroxylation	($-CH_2$+O)	1.9793	208.9939
Ketone to alcohol	($+H_2$)	2.0157	209.0303
Methylene to ketone	($-H_2$+O)	13.9793	220.9939

Table 4.2. Exact mass (m/z) of the expected metabolites of HCA……*Continued*

Metabolism Reaction	Formula change	Accurate mass change	Accurate mass
Hydroxylation and desaturation	(-H_2+O)	13.9793	220.9939
Hydroxylation	(+O)	15.9949	223.0095
Demethylation and Two hydroxylation	(-CH_2+O_2)	17.9742	224.9888
Hydration/hydrolysis	(+H_2O)	18.0106	225.0252
Hydroxylation and ketone formation	(-H_2+O_2)	29.9742	236.9888
Two hydroxylation	(+O_2)	31.9898	239.0044
Three hydroxylation	(+O_3)	47.9847	254.9993
O-dealkylation	(-C_4H_8O)	(-72.0575)	134.9575
Hydroxy acid	(-H_2+O_2)	29.9741	236.9887
Methylation	(+CH_2)	14.0157	221.0303
Hydroxylation and methylation	(+CH_2O)	30.0105	237.0251
Acetylation	(+C_2H_2O)	42.0106	249.0252
Glycine conjugation	(+C_2H_3NO)	57.0215	264.0361
Sulfation	(+SO_3)	79.9568	286.9714
Hydroxylation and sulfation	(+SO_4)	95.9517	302.9663
Cysteine conjugation	(+C_3H_5NOS)	103.0092	310.0238
Taurine conjugation	(+$C_2H_5NO_2S$)	107.0041	314.0187
S-cysteine conjugation	(+$C_3H_5NO_2S$)	119.0041	326.0187
Decarboxylation and glucuronidation	(+$C_5H_8O_5$)	148.0372	355.0518
Two sulfate conjugation	(+S_2O_6)	159.9136	366.9282
N-acetylcysteine conjugation	(+$C_5H_7NO_3S$)	161.0147	368.0293
S-cysteinylglycine conjugation	(+$C_5H_8N_2O_3S$)	176.0256	383.0401
Glucuronidation	(+$C_6H_8O_6$)	176.0321	383.0467
Hydroxylation and glucuronidation	(+$C_6H_8O_7$)	192.0273	399.0416
GSH conjugation	(+$C_{10}H_{17}N_3O_5S$)	291.0889	498.1035
Desaturation and S-GSH conjugation	(+$C_{10}H_{17}N_3O_5S$)	305.0682	512.0828
S-GSH conjugation	(+$C_{10}H_{17}N_3O_5S$)	307.0838	514.0984
Epoxidation and S-GSH conjugation	(+$C_{10}H_{17}N_3O_5S$)	323.0787	530.0933
Two glucuronide conjugation	(+$C_{12}H_{16}O_{12}$)	352.0664	559.0812

However, there was only 1 direct glucuronidated metabolite found in the incubation mixture (Table 4.3) and no phase I metabolite was observed from rat liver RLS9 fraction.

Table 4.3. Metabolite of HCA obtained after incubation in RLS9.

No.	$[M-H]^-$ m/z	Mass error (PPM)	MS^2 Fragment ions	Metabolite description
M1	383.0452	-3.9	383.0452, 207.0142, 127.0401	Glucuronidation

The only direct glucuronide metabolite M1 (m/z: 383.0452) showed the typical fragment ions at m/z 207.0142 (loss of a glucuronic acid unit) and 127.0401 (HCA fragment ion). Therefore, M1 was determined as a mono-glucuronidated metabolite of HCA. As HCA is quite a polar molecule, it is expected to get eliminated from the body without any modification by the body. Due to its polar nature, it may not be accessible to drug-metabolizing enzymes.

4.2.2. QCN

In-silico Analysis of Metabolism of QCN

Table 4.4 shows the *in-silico* prediction of metabolites of QCN using ADMET Predictor® of GastroPlus® and depicts the mass of potential metabolites through the listed enzymes.

Table 4.4. Output of ADMET Predictor® for metabolite prediction of QCN.

Identifier	Metabolizing enzyme	Mass
QCN		302.242
QCN - M1	UGT1A1;UGT1A3;UGT1A8;UGT1A9; UGT1A10;UGT2B7	478.0741
QCN - M2	UGT1A1;UGT1A3;UGT1A8;UGT1A9; UGT1A10;UGT2B7	478.0741
QCN - M3	UGT1A1;UGT1A3;UGT1A8;UGT1A9;UGT1A10; UGT2B7	478.0741
QCN - M4	UGT1A1;UGT1A3;UGT1A8;UGT1A9;UGT1A10; UGT2B7	478.0741
QCN - CypM1		318.241
QCN - CypM1 - M1	UGT1A1;UGT1A3;UGT1A8;UGT1A9;UGT1A10; UGT2B7	494.0690
QCN - CypM1 - M2	UGT1A1;UGT1A3;UGT1A8;UGT1A9;UGT1A10; UGT2B7	494.0690
QCN - CypM1 - M3	UGT1A1;UGT1A3;UGT1A8;UGT1A9;UGT1A10; UGT2B7	494.0690
QCN - CypM1 - M4	UGT1A3;UGT1A8;UGT1A10;UGT2B7	494.0690
QCN - CypM1 - M5	UGT1A3;UGT1A8;UGT1A10;UGT2B7	494.0690
QCN - CypM2		316.225
QCN - CypM2 - M1	UGT1A1;UGT1A3;UGT1A8;UGT1A9;UGT1A10; UGT2B7	492.0534
QCN - CypM2 - M2	UGT1A1;UGT1A3;UGT1A8;UGT1A9;UGT1A10; UGT2B7	492.0534

Direct glucuronidation, oxidation and dehydrogenated oxidation are predicted to be the major primary metabolites of QCN. The oxidative metabolites are predicted to undergo further glucuronidation. On the similar lines, Oliveira and Watson reported that QCN was extensively metabolized by UGT1A9 [9].

Metabolite Identification of QCN in RLS9

The incubation protocol is described in Section 3.4. . Briefly, the final concentration of the protein was 1 mg/mL (RLS9 fraction), and QCN concentration was 10 μg/mL. Control incubations did not had QCN/NADPH. After a pre-incubation period of 5 minutes at 37 °C, addition of 2.0 mM NADPH cofactor solution instigated the metabolic reaction. Subsequent to the incubation for 60 minutes, 1 mL ice-cold acetonitrile was added to the reaction mixture to quench the same, and the resultant samples were subjected to centrifugation at 10,000 rpm for 10 minutes before injecting on to the HRMS.

Mass Fragment Ions of QCN

Using QCN as the basic core for its metabolites, the MS^2 fragment ions can be used as a guide for metabolite identification. In the MS^2 mode, when the collision energy was set at 22 eV, QCN yielded ample fragment ions at m/z 178.9981 (Theoretical m/z: 178.9986, $C_8H_3O_5$, -2.8 ppm), 121.0287 (Theoretical m/z: 121.0295, $C_7H_5O_2$, -6.6 ppm), 151.0031 (Theoretical m/z: 151.0037, $C_7H_3O_4$, -4.0 ppm), and 149.0237 (Theoretical m/z: 149.0244, $C_8H_5O_3$, -4.7 ppm) through cleavage of the ring (Figure 4.2).

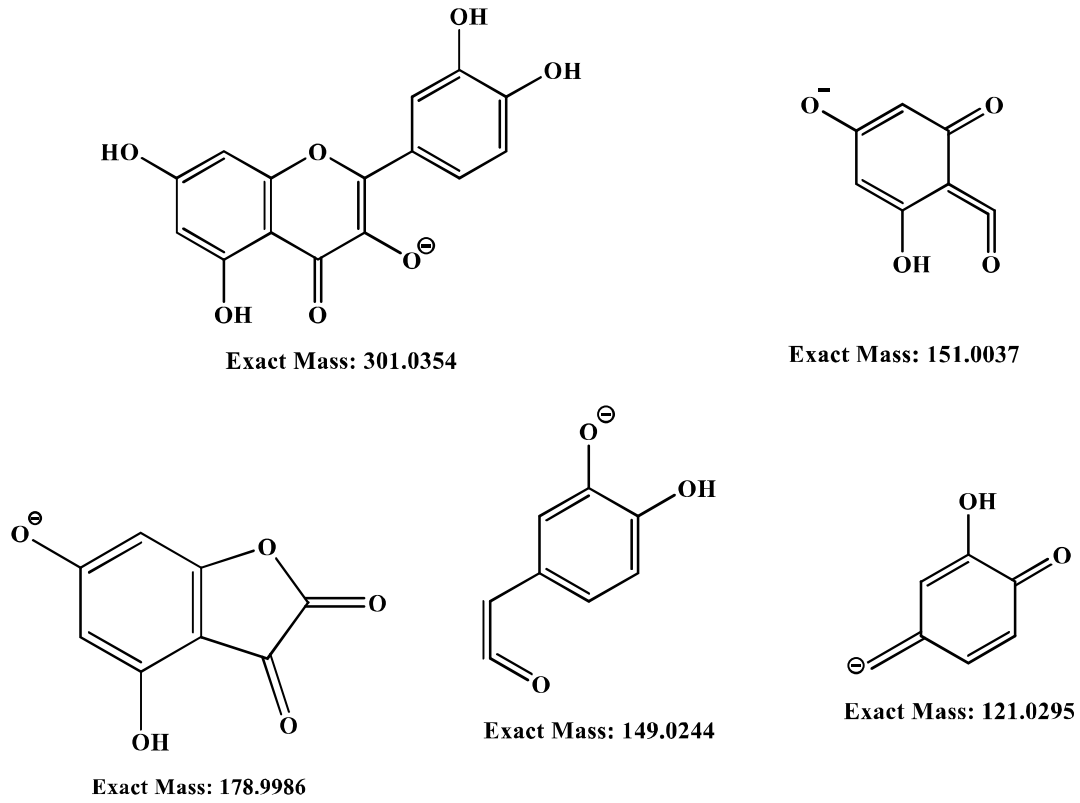

Figure 4.2. Predicted (theoretical) mass fragmentation ions of QCN

A template was prepared based on the accurate mass of metabolites to quickly search and identify corresponding metabolites for the compounds used in the studies. Table 4.5 depicts

such a template for QCN for phase I and phase II metabolites. This mass list was used to acquire a data-dependent scan on HRMS.

Table 4.5. Exact mass (m/z) of the expected metabolites of QCN.

[M-H]-	301.0354		
Metabolism Reaction	**Formula change**	**Accurate mass change**	**Accurate mass**
ter-butyl dealkylation	($-C_4H_8$)	(-56.0626)	244.9728
Decarboxylation	($-CO_2$)	(-43.9898)	257.0456
Isopropyl dealkylation	($-C_3H_6$)	(-42.047)	258.9884
Reductive dechlorination	(+H-Cl)	(-33.961)	267.0744
Deethylation	($-C_2H_4$)	(-28.0313)	273.0041
Reductive defluorination	(+H-F)	(-17.9906)	283.0448
Oxidative dechlorination	(+OH-Cl)	(-17.9661)	283.0693
Demethylation	($-CH_2$)	(-14.0157)	287.0197
Two sequential desaturations	($-H_4$)	(-4.0313)	297.0041
Hydroxylation and dehydration	($-H_2$)	(-2.0157)	299.0197
Alcohol to ketone/aldehyde	($-H_2$)	(-2.0157)	299.0197
Desaturation	($-H_2$)	(-2.0157)	299.0197
Oxidative defluorination	(+OH-F)	(-1.9957)	299.0397
Oxidative deamination	($-NH_3$+O)	(-1.0316)	300.0038
Demethylation and hydroxylation	($-CH_2$+O)	1.9793	303.0147
Ketone to alcohol	($+H_2$)	2.0157	303.0511
Methylene to ketone	($-H_2$+O)	13.9793	315.0147
Hydroxylation and desaturation	($-H_2$+O)	13.9793	315.0147
Hydroxylation	(+O)	15.9949	317.0303
Demethylation and Two hydroxylation	($-CH_2+O_2$)	17.9742	319.0096
Hydration/hydrolysis	($+H_2O$)	18.0106	319.046
Hydroxylation and ketone formation	($-H_2+O_2$)	29.9742	331.0096
Two hydroxylation	($+O_2$)	31.9898	333.0252
Three hydroxylation	($+O_3$)	47.9847	349.0201
o-dealkylation	($-C_4H_8O$)	(-72.0575)	228.9775
Hydroxy acid	($-H_2+O_2$)	29.9746	331.0095
Methylation	($+CH_2$)	14.0157	315.0511
Hydroxylation and methylation	($+CH_2O$)	30.0105	331.0459
Acetylation	($+C_2H_2O$)	42.0106	343.0461
Glycine conjugation	($+C_2H_3NO$)	57.0215	358.0569
Sulfation	($+SO_3$)	79.9568	380.9922
Hydroxylation and sulfation	($+SO_4$)	95.9517	396.9871
Cysteine conjugation	($+C_3H_5NOS$)	103.0092	404.0446
Taurine conjugation	($+C_2H_5NO_2S$)	107.0041	408.0395
S-cysteine conjugation	($+C_3H_5NO_2S$)	119.0041	420.0395
Decarboxylation and glucuronidation	($+C_5H_8O5$)	148.0372	449.0726

Table 4.5. Exact mass (m/z) of the expected metabolites of QCN……. *Continued*

Metabolism Reaction	Formula change	Accurate mass change	Accurate mass
Two sulfate conjugation	(+S_2O_6)	159.9136	460.9491
N-acetylcysteine conjugation	(+$C_5H_7NO_3S$)	161.0147	462.0501
S-cysteinylglycine conjugation	(+$C_5H_8N_2O_3S$)	176.0256	477.0606
Glucuronidation	(+$C_6H_8O_6$)	176.0321	477.0675
Hydroxylation and glucuronidation	(+$C_6H_8O_7$)	192.0271	493.0624
GSH conjugation	(+$C_{10}H_{17}N_3O_5S$)	291.0889	592.1243
Desaturation and S-GSH conjugation	(+$C_{10}H_{17}N_3O_5S$)	305.0682	606.1036
S-GSH conjugation	(+$C_{10}H_{17}N_3O_5S$)	307.0838	608.1192
Epoxidation and S-GSH conjugation	(+$C_{10}H_{17}N_3O_5S$)	323.0787	624.1141
Two glucuronide conjugation	(+$C1_2H_{16}O_{12}$)	352.0664	653.1018
Glutathione substitution dealkylation glucuronidation	($C_1H_8N_3O_5S$)	173.0106	474.0460

Overall, 31 metabolites were found in the incubation mixture, that comprised of various phase II metabolites including methylation, glucuronidation and sulfation transformations (details of metabolites are provided in Table 4.6). Even direct glutathione adducts were observed suggesting that the dose of QCN might play an important role in deciding the metabolism and toxicity of this compound.

Table 4.6. Metabolites of QCN obtained after incubation in RLS9.

No.	$[M-H]^-$ m/z	Mass error (PPM)	MS/MS Fragment ions	Metabolite description
M1	653.0987	-4.7	653.0987, 477.0669, 301.0354	Di-glucuronidation
M2	653.0989	-4.4	653.0989, 477.0669, 301.0353	Di-glucuronidation
M3	653.0998	-3.1	653.0998, 477.0670, 301.0352	Di-glucuronidation
M4	303.0508	-0.99	303.0508, 285.0397, 178.9981	Reduction
M5	317.0659	-2.8	317. 0659, 303.0509, 285.0399	Reduction & Methylation
M6	477.0668	-1.5	477.0668, 301.0352, 151.0038	Glucuronidation
M7	477.0669	-1.2	477.0669, 301.0354, 151.0038	Glucuronidation
M8	477.0667	-1.7	477.0667, 301.0354, 151.0037	Glucuronidation
M9	477.0667	-1.7	477.0667, 301.0354, 151.0038	Glucuronidation
M10	343.0449	-3.5	343.0449, 301.0354, 151.0037	Acetylation

Table 4.6. Metabolites of QCN obtained after incubation in RLS9…… *Continued*

No.	$[M-H]^-$	Mass error (PPM)	MS/MS Fragment ions	Metabolite description
M11	315.0509	-0.6	315.0509, 301.0354, 151.0037	Methylation
M12	315.0501	-3.7	315.0501, 301.0354, 151.0037	Methylation
M13	329.0662	-1.8	329.0662, 315.0511, 301.0354	Dimethylation
M14	491.0821	-2.2	491.0821, 315.0510, 301.0354	Glucuronidation & Methylation
M15	491.0824	-1.6	491.0824, 315.0511, 301.0353	Glucuronidation & Methylation
M16	491.0825	-1.4	491.0825, 315.0511, 301.0354	Glucuronidation & Methylation
M17	491.0826	-1.2	491.0826, 315.0511, 301.0352	Glucuronidation & Methylation
M18	491.0827	-1.0	491.0827, 315.0512, 301.0353	Glucuronidation & Methylation
M19	491.0823	-1.8	491.0823, 315.0512, 301.0353	Glucuronidation & Methylation
M20	667.1156	-2.8	667.1156, 491.0831, 315.0511	Diglucuronidation & Methylation
M21	667.1157	-2.7	667.1157, 491.0832, 315.0511	Diglucuronidation & Methylation
M22	505.0985	-0.79	505.0985, 491.0832, 315.0511, 301.0354	Glucuronidation & Dimethylation
M23	380.9920	-0.52	380.9920, 301.0354, 151.0037	Sulfation
M24	380.9921	-0.26	380.9921, 301.0354, 151.0037	Sulfation
M25	395.0074	-1.26	395.0074, 380.9922, 301.0354	Methylation & Sulfation
M26	395.0077	-0.5	395.0077, 380.9922, 301.0354	Methylation & Sulfation
M27	571.0396	-0.7	571.0396, 491.0832, 315.0511, 301.0354	Glucuronidation & Methylation & Sulfation
M28	606.1043	1.1	606.1043, 299.0198	Glutathione
M29	606.1051	2.5	606.1051, 299.0198	Glutathione
M30	606.1026	-1.6	606.1026, 299.0198	Glutathione
M31	606.1034	-3.3	606.1034, 299.0198	Glutathione

PPM: parts per million; to denote mass error during high-resolution mass spectrometry analysis

As indicated in Table 4.6, M1, M2 and M3 (Theoretical m/z: 653.1018 and observed m/z were within 5 ppm) generated characteristic fragment ions at m/z 477.0669 (loss of a moiety of glucuronic acid) and 301.0354 (loss of both glucuronic acids). Therefore, M1, M2 and M3 were determined as di-glucuronidation adducts of QCN.

M4 was a reduction metabolite through the addition of hydrogen. Parent ion [M–H]- of M4

was 303.0508 (Theoretical m/z: 303.0511, ppm error: -0.99). In its product ion spectra, [M-H] ion showed fragment ions at *m/z* 285.0397 (loss of H_2O) and 178.9981 (loss of $C_7H_8O_2$ fragment ion). M5 with an m/z: 317.0659 (Theoretical m/z: 317.0668, ppm error: -2.8), showed MS/MS spectra, *m/z* 303.0509 (loss of CH_2) and 285.0399 (loss of CH_2 and H_2O), suggesting M5 was proposed to be the reduction and methylated metabolite of QCN.

Four metabolites M6, M7, M8 and M9 (Theoretical m/z: 477.0765 and observed m/z were within 2 ppm) yielded characteristic fragment ions at m/z 301.0354 (corresponding to the loss of glucuronic acid moiety) and 151.0037 (QCN fragment ion). Therefore, M6, M7, M8 and M9 were determined as glucuronidation adducts of QCN.

M10 with an *m/z* 343.0449 (Theoretical m/z: 343.0461, ppm error: -3.5) yielded characteristic fragment ions at m/z 301.0354 (loss of acetyl group) and 151.0037 (QCN fragment ion). Therefore, M10 was assigned to be an acetylated form of QCN.

Two metabolites, M11 and M12 (Theoretical m/z: 315.0511 and observed m/z were within mass error of 4 ppm) yielded characteristic fragment ions at m/z 301.0354 (loss of methyl group) and 151.0037 (QCN fragment ion). Therefore, M11 and M12 were assigned as methylated adducts of QCN. M13 (Theoretical m/z: 329.0668, ppm error: -1.8) yielded fragment ion of 315.0511 (loss of one methyl group) and 301.0354 (loss of both methyl groups), hence, was assigned as a dimethylated metabolite of QCN.

Six metabolites namely M14, M15, M16, M17, M18 and M19 (Theoretical m/z: 491.0832 and observed m/z within mass error of 3 ppm) yielded characteristic fragment ions at m/z 315.0511 (loss of methyl group) and 301.0534 (loss of methyl and glucuronic acid moiety). Therefore, M14, M15, M16, M17, M18 and M19 were assigned as methylated and mono-glucuronidated metabolites of QCN.

M20 and M21 (Theoretical m/z: 667.1175 and observed m/z within mass error of 3 ppm) yielded fragment ions 491.0832 (loss of glucuronic acid moiety), 315.0511 (loss of both glucuronic acid moieties). Hence, M20 and 21 were proposed to be diglucuronidated and mono-methylated adducts of QCN.

M22 (Theoretical m/z: 505.0989, mass error: -1.8 ppm) yielded fragment ions 491.0832 (loss of methyl moiety), 315.0511 (loss of glucuronic acid and one methyl group) and 301.0354 (loss of one glucuronic acid and two methyl moieties) and hence was assigned to be a mono-glucuronidated and dimethylated metabolite of QCN.

M23 and M24 (Theoretical m/z: 380.9922 and observed m/z well within 1 ppm) yielded fragment ions 301.0354 (loss of sulfate moiety) and 151.0037 (QCN fragment ion). Hence, M23 and M24 were estimated to be sulfate adducts of QCN. M25 and M26 (Theoretical m/z:

395.0079 and observed m/z within 2 ppm) yielded fragment ions 380.9922 (loss of methyl moiety) and 301.0354 (loss of methyl and sulfate group), therefore, the two were anticipated to be sulfated and methylated adducts of QCN, respectively.

M27 (Theoretical m/z: 571.0400, ppm error: -0.7) fragmented to 491.0832 (loss of sulfate moiety), 315.0511 (loss of glucuronic acid and sulfate moiety) and 301.0354 (loss of glucuronic acid, sulfate and methyl moieties). Hence, M27 was assigned to be glucuronidated, methylated & sulfated metabolite. M28-M31 (Theoretical m/z: 606.1036, ppm error: within 4 ppm) are direct glutathione adducts of QCN that fragmented to yield dehydrogenated quercetin fragment (m/z: 299.0198). Hence, M28-31 were assigned to be glutathione adducts.

4.2.3. GLZ

In-silico Analysis of Metabolism of GLZ

Table 4.7 shows the *in-silico* prediction of GLZ using ADMET Predictor® of GastroPlus® and depicts the mass of potential metabolites through the listed enzymes.

Table 4.7. Output of ADMET Predictor® for metabolite prediction of GLZ

Identifier	Metabolizing enzyme(s)	Mass
Glycyrrhizin		**822.951**
GLZ- M1	UGT1A3	998.4338
GLZ- M2	UGT1A3	998.4338
GLZ- M3	UGT1A3	998.4338
GLZ- M4	UGT1A3	998.4338
GLZ- M5	UGT1A3	998.4338
GLZ- M6	UGT2B7	998.4338
GLZ- M7	UGT2B7	998.4338
GLZ- M8	UGT2B7	998.4338

One of the major metabolites for GLZ is GA, which further undergoes secondary metabolism. Table 4.8 shows the *in-silico* prediction of GA using ADMET Predictor® of GastroPlus® and depicts the mass of potential metabolites through the listed enzymes.

Table 4.8. Output of ADMET Predictor® for metabolite prediction of GA.

Identifier	Metabolizing Enzyme(s)	Molecular weight
GA		470.697
GA - M1	UGT1A3	646.3702
GA - M2	UGT2B7	646. 3702

Table 4.8. Output of ADMET Predictor® for metabolite prediction of GA….. *Continued*

Identifier	Metabolizing Enzyme(s)	Molecular weight
GA - CypM1		468.681
GA - CypM1 - M1	UGT1A3;UGT2B7	644.3546
GA - CypM2		486.697
GA - CypM2 - M1	UGT1A3	662.3651
GA - CypM2 - M2	UGT1A3	662.3651
GA - CypM2 - M3	UGT2B7	662.3651
GA - CypM3		486.697
GA - CypM3 - M1	UGT1A3	662.3651
GA - CypM3 - M2	UGT1A3	662.3651
GA - CypM3 - M3	UGT2B7	662.3651
GA - CypM4		486.697
GA - CypM4 - M1	UGT1A3	662.3651
GA - CypM4 - M2	UGT1A3	662.3651
GA - CypM4 - M3	UGT2B7	662.3651
GA - CypM5		486.697
GA - CypM5 - M1	UGT1A3	662.3651
GA - CypM5 - M2	UGT2B7	662.3651
GA - CypM6		486.697
GA - CypM6 - M1	UGT1A3	662.3651
GA - CypM6 - M2	UGT2B7	662.3651
GA - CypM7		486.697
GA - CypM7 - M1	UGT1A3	662.3651
GA - CypM7 - M2	UGT2B7	662.3651

GLZ is predicted to undergo de-diglucuronidation to form GA. GA is predicted to go through further metabolism including dehydrogenation and oxidation. These metabolites are predicted to be liable to further glucuronidation.

Metabolite identification of GLZ in RLS9

The incubation protocol is described in Section 3.4. Briefly, the final concentration of the protein was 1 mg/mL (RLS9 fraction), and GLZ concentration was 10 μg/mL. Control incubations did not had GLZ/NADPH. After a pre-incubation period of 5 minutes at 37 °C, addition of 2.0 mM NADPH cofactor solution instigated the metabolic reaction. Subsequent to the incubation for 60 minutes, 1 mL ice-cold acetonitrile was added to the reaction mixture to quench the same, and the resultant samples were subjected to centrifugation at 10,000 rpm for 10 minutes before injecting on to the HRMS.

Mass fragment ions of GLZ

Using GLZ as the central core, the MS^2 fragment ions could be used as indicators for metabolite identification. In the MS/MS mode, the collision energy was of 35 eV, yielded fragment ions at *m/z* 453.3363 and *m/z* 471.3469. Enzymatic hydrolysis of GLZ happens in the intestine to form GA. The GA shows a typical loss of 44 ($-CO_2$) to give a fragment ion of 425.3425. The fragmentation ions of GLZ and GA are shown in Figure 4.3.

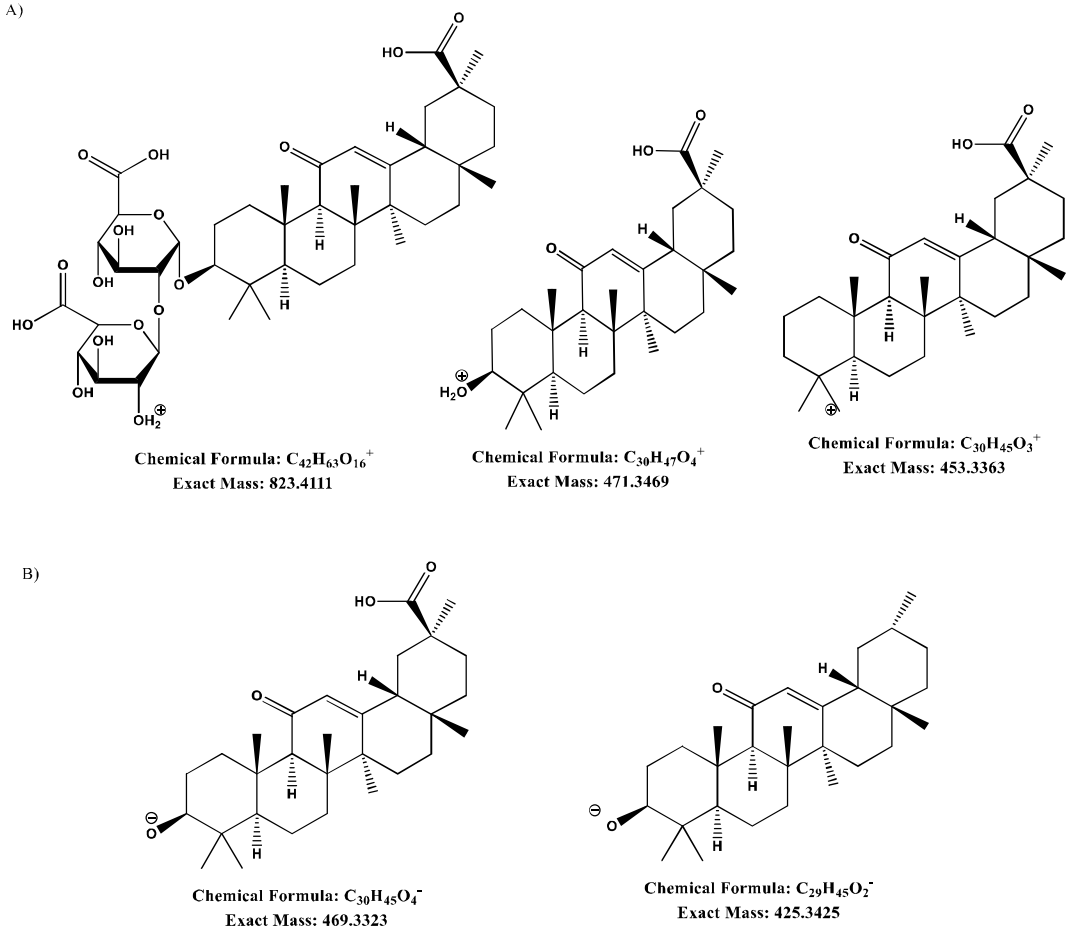

Figure 4.3. Predicted (theoretical) mass fragmentation ions of GLZ (A) and GA(B)

Based on molecular weight, the exact masses of the metabolites of GLZ and GA are presented in Table 4.9.

Table 4.9. Exact mass (m/z) of the expected metabolites of GLZ and GA.

GLZ [M+H]+	823.4111		GA [M-H]-	469.3323
Metabolism reaction	**Formula change**	**Accurate mass change**	**Accurate mass (GLZ)**	**Accurate mass (GA)**
ter-butyl dealkylation	($-C_4H_8$)	(-56.0626)	767.3485	413.2697
Decarboxylation	($-CO_2$)	(-43.9898)	779.4213	425.3425
Isopropyl dealkylation	($-C_3H_6$)	(-42.047)	781.3641	427.2853
Reductive dechlorination	(+H-Cl)	(-33.961)	789.4501	435.3713

Table 4.9. Exact mass (m/z) of the expected metabolites of GLZ and GA ….*Continued*

Metabolism reaction	Formula change	Accurate mass change	Accurate mass (GLZ)	Accurate mass (GA)
Deethylation	(-C_2H_4)	(-28.0313)	795.3798	441.3011
Demethylation	(-CH_2)	(-14.0157)	805.4205	455.3166
Two sequential desaturations	(-H_4)	(-4.0313)	805.4450	465.3011
Hydroxylation and dehydration	(-H_2)	(-2.0157)	809.3954	467.3166
Alcohol to ketone/aldehyde	(-H_2)	(-2.0157)	819.3798	467.3166
Desaturation	(-H_2)	(-2.0157)	821.3954	467.3166
Oxidative defluorination	(+OH-F)	(-1.9957)	821.3954	467.3366
Oxidative deamination	(-NH_3+O)	(-1.0316)	821.3954	468.3007
Demethylation and hydroxylation	(-CH_2+O)	1.9793	821.4154	471.3116
Ketone to alcohol	(+H_2)	2.0157	822.3795	471.3481
Methylene to ketone	(-H_2+O)	13.9793	825.3904	483.3116
Hydroxylation and desaturation	(-H_2+O)	13.9793	825.4268	483.3116
Hydroxylation	(+O)	15.9949	837.3904	485.3272
Demethylation and Two hydroxylation	(-CH_2+O_2)	17.9742	837.3904	487.3065
Hydration/hydrolysis	(+H_2O)	18.0106	839.4060	487.3429
Hydroxylation and ketone formation	(-H_2+O_2)	29.9742	841.3853	499.3065
Two hydroxylation	(+O_2)	31.9898	841.4217	501.3221
Three hydroxylation	(+O_3)	47.9847	853.3853	517.3172
o-dealkylation	(-C_4H_8O)	(-72.0575)	855.4009	397.2747
Hydroxy acid	(-H_2+O_2)	29.9741	871.3958	499.3064
Methylation	(+CH_2)	14.0157	837.4268	483.3481
Hydroxylation and methylation	(+CH_2O)	30.0105	853.4216	499.3428
Acetylation	(+C_2H_2O)	42.0106	865.4217	511.3429
Glycine conjugation	(+C_2H_3NO)	57.0215	880.4326	526.3538
Sulfation	(+SO_3)	79.9568	903.3679	549.2891
Hydroxylation and sulfation	(+SO_4)	95.9517	919.3628	565.2841
Cysteine conjugation	(+C_3H_5NOS)	103.0092	926.4203	572.3415
Taurine conjugation	(+$C_2H_5NO_2S$)	107.0041	930.4152	576.3364
S-cysteine conjugation	(+C3H5NO2S)	119.0041	942.4152	588.3364
Decarboxylation and glucuronidation	(+$C_5H_8O_5$)	148.0372	971.4483	617.3695

Table 4.9. Exact mass (m/z) of the expected metabolites of GLZ and GA ….*Continued*

Metabolism reaction	Formula change	Accurate mass change	Accurate mass (GLZ)	Accurate mass (GA)
Two sulfate conjugation	(+S_2O_6)	159.9136	983.3247	629.2459
N-acetylcysteine conjugation	(+$C_5H_7NO_3S$)	161.0147	984.4258	630.347
S-cysteinylglycine conjugation	(+$C_5H_8N_2O_3S$)	176.02556	999.43666	645.35786
Glucuronidation	(+$C_6H_8O_6$)	176.0321	999.4432	645.3644
Hydroxylation and glucuronidation	(+$C_6H_8O_7$)	192.027	1015.4381	661.3593
GSH conjugation	(+$C_{10}H_{17}N_3O_5S$)	291.0889	1114.5	760.4212
Desaturation and S-GSH conjugation	(+$C_{10}H_{15}N_3O_6S$)	305.0682	1128.4793	774.4005
S-GSH conjugation	(+$C_{10}H_{17}N_3O_6S$)	307.0838	1130.4949	776.4161
Epoxidation and S-GSH conjugation	(+$C_{10}H_{17}N_3O_7S$)	323.0787	1146.4898	792.411
Two glucuronide conjugation	(+$C_{12}H_{16}$O12)	352.06642	1175.47752	821.39872
Glutathione substitution dealkylation glucuronidation	($C_1H_8N_3O_5S$)	173.01067	996.42177	642.34297

There was no GLZ found in the incubation mixture. The major metabolite was found to be the de-diglucuronidated (GA) that further undergoes glucuronidation and sulfation (Table 4.10).

Table 4.10. Metabolites of GA obtained after incubation in RLS9

No.	$[M-H]^-$ m/z	Mass error (PPM)	MS^2Fragment ions	Metabolite description
M1	645.3648	0.6	469.3323, 425.3425	Glucuronidation
M2	511.3425	-0.7	469.3321, 425.3424	Acetylation
M3	821.3985	-0.2	645.3645, 469.3321, 425.3425	Diglucuronidation
M4	549.2889	-0.36	469.3322, 425.3426	Sulfation

M1 (Theoretical m/z: 645.3644, ppm error: 0.6) yielded characteristic fragment ions at m/z 469.3323 (loss of glucuronic acid) and 425.3425 (fragment of GA). Therefore, M1 was assigned to be a mono-glucuronidated metabolite of GA. M2 (Theoretical m/z: 511.3429, ppm error: -0.7) yielded characteristic fragment ions at m/z 469.3321 (loss of acetyl group) and 425.3424 (fragment of GA). Hence, M2 was proposed to be a mono-acetylated metabolite of GA. Peak corresponding to m/z 821.3985 was assigned to be M3, which showed the characteristic fragment of 645.3645 (loss of one glucuronic acid moiety), 469.3321 (loss of two glucuronic acid moieties) and 425.3425 (fragment of GA) suggesting that M3 is a di-glucuronidated metabolite of GA. M4 (Theoretical m/z: 549.2889, ppm error: -0.36) yielded characteristic fragment ions at m/z 469.3322 (loss of sulfate moiety) and 425.3426 (fragment

of GA). Therefore, M4 was assigned to be a mono-sulfated metabolite of GA.

4.3. Conclusion

The *in silico* and *in vitro* metabolite identification of QCN, GLZ and HCA were carried out. The data from both set of studies suggest that conjugation reactions are the main mode of metabolism instead of CYPs. QCN underwent through high metabolism and a total of 31 metabolites were observed when it was incubated in freshly isolated RLS9 fraction. HCA exhibited minimal metabolism and only one direct glucuronidated metabolite was observed. This is the first report on the metabolism of HCA. GLZ was completely converted to GA, which further underwent phase II metabolic reactions and yielded glucuronidated, di-glucuronidated, acetylated and sulphated metabolites

References

1. P. Baranczewski, A. Stanczak, K. Sundberg, R. Svensson, A. Wallin, J. Jansson, P. Garberg and H. Postlind. Introduction to *in vitro* estimation of metabolic stability and drug interactions of new chemical entities in drug discovery and development. Pharmacol Rep 58 (2006) 453-472.
2. U.A. Meyer. Overview of enzymes of drug metabolism. J Pharmacokin Biopharm 24 (1996) 449-459.
3. S. Rendic, Summary of information on human CYP enzymes: human P450 metabolism data. Drug Met Rev 34 (2002) 83-448.
4. G.N. Kumar and S. Surapaneni. Role of drug metabolism in drug discovery and development. Med Res Rev 21 (2001) 397-411.
5. U.A. Argikar, P.M. Potter, J.M. Hutzler and P.H. Marathe. Challenges and opportunities with non-CYP enzymes aldehyde oxidase, carboxylesterase, and UDP-lucuronosyltransferase: focus on reaction phenotyping ad prediction of human clearance. The AAPS Journal 18 (2016) 1391-1405.
6. S. Ekins, B.J. Ring, J. Grace, D.J. McRobie-Belle and S.A. Wrighton. Present and future *in vitro* approaches for drug metabolism. J Pharmacol Toxicol Methods 44 (2000) 313-324.
7. S. Alqahtani. *In silico* ADME-Tox modeling: progress and prospects. Expert Opin Drug Metab Toxicol 13 (2017) 1147-1158.
8. K. Sakaguchi, M. Green, N. Stock, T.S. Reger, J. Zunic and C. King. Glucuronidation of carboxylic acid containing compounds by UDP-glucuronosyltransferase isoforms. Arch Biochem Biophy 424 (2004) 219-225.
9. E.J. Oliveira and D.G. Watson. *In vitro* glucuronidation of kaempferol and QCN by human UGT-1A9 microsomes. FEBS Lett 471 (2000) 1-6.